Chapter 16
Multi-model Approach for Spatial Evapotranspiration Mapping: Comparison of Models Performance for Different Ecosystems

Temesgen Enku, Christiaan van der Tol, Assefa M. Melesse, Semu A. Moges and A. Gieske

Abstract Accurate estimation of evapotranspiration (ET) is vital for water resource management. The FAO-56 Penman–Monteith (FAO-56 PM) is a standard method, but it requires numerous weather data. This challenges water resource managers to estimate ET in areas where there are no adequate meteorological data. Hence, simplified approaches that are less data intensive are the right alternatives. Here, ET was estimated using different approaches and their performances were evaluated in different ecosystems of Ethiopia. Surface Energy Balance Systems (SEBS) model was also used for spatio-temporal mapping of ET in the Fogera floodplain, Lake Tana Basin. The spatial average of actual ET (ETa) from remote-sensing (RS) data over the floodplain was less than the Penman–Monteith (PM) reference ET (ETo) in drier periods and larger in wet seasons. A sensitivity analysis of PM input variables at the Bahir Dar station showed that the incoming solar radiation and air temperature are most sensitive, and wind speed was found to be the least sensitive. The comparison of simple Enku (E) temperature method, Abtew (A) equation, modified Makkink

T. Enku (✉)
School of Civil and Water Resources Engineering,
Bahir Dar University, Bahir Dar, Ethiopia
e-mail: temesgenku@gmail.com

C. v. d. Tol · A. Gieske
Department of Water Resources,
Faculty of geo-information Science and Earth Observation (ITC), University of Twente,
Enschede, The Netherlands
e-mail: tol@utwente.nl

A. Gieske
e-mail: gieske@utwente.nl

A. M. Melesse
Department of Earth and Environment,
Florida International University, Miami, FL, USA
e-mail: melessea@fiu.edu

S. A. Moges
Department of Civil Engineering, Addis Ababa University, Addis Ababa, Ethiopia
e-mail: semu_moges_2000@yahoo.com

(MM) method, and Priestley–Taylor (PT) method with the PM ETo in the different ecosystems of Ethiopia showed the MM method performed best in all the stations except Dire Dawa stations with coefficient of determination (R^2) of 0.94, Nash–Sutcliffe efficiency (NSE) of 0.88, root mean square error (RMSE) of 0.26 mm, and absolute mean error (AME) of 0.21 mm at Addis Ababa and Awassa stations. The performance of MM and PT methods in the dry and hot climate was poor. The E method performed consistently well in all the stations considered. While ET estimation from remotely sensed inputs has generally been improved, selection of the method of estimation is very important and should always be tested with observational data.

16.1   Introduction

Population growth over the past decades and the economic growth in Ethiopia caused the demand for freshwater to increase. Water supply has to meet requirements not only for irrigation and agricultural production but also for domestic uses. Hence, well-planned and adequate water resources management is required at local and regional scales in East Africa. For such management, quantitative assessments need to be made for meteorological processes of precipitation and evapotranspiration (ET) that affect the water balance of the basins at large. ET and precipitation are the inputs to most hydrological models for studying water resource planning and management, assessment of irrigation efficiency of existing projects, evaluation of future drainage requirements, design of reservoirs and reservoir operations, water supply requirements of proposed irrigation projects, water supply requirements for domestic purposes, and preparation of river forecasts, to name but a few. There exist a multitude of methods, for estimation of ET. The availability of many methods for determining ET, with the wide range of data types needed, makes it difficult to select the most appropriate method from a group of methods for a given agro-climatic regions. There is, therefore, a need to analyze and compare the various existing ET models. Therefore, the objectives of this study are to (1) estimate actual ET (ETa) on the Fogera floodplain, Lake Tana basin, that probably is the most productive agricultural area in the Lake Tana basin, (2) estimate reference ET (ETo) using different empirical methods at different ecosystems and compare their performance with the more complete Penman–Monteith (PM) method, and (3) understand the most sensitive weather variable inputs to the PM ETo estimate in the area.

16.2   Study Area

Ethiopia is found in the horn of Africa; it lies between about 3°N to 15°N and 33°E to 48°E. The altitude in Ethiopia ranges from a lower elevation of about 116 m below sea level, in the Dallol depression of the Afar region, northeastern part of the country, to a highest elevation of about 4,620 m above sea level at Ras Dashen, in the Semien Mountains in the northern part of the country. Due to this high altitude difference, there is considerable spatial variability of temperature and climate, whereas seasonal variability is relatively low. Ethiopia is subdivided into five climatic regimes: moist, dry subhumid, semiarid, arid, and hyperarid regimes.

The Ethiopian National Meteorological Agency (ENMA) defines three seasons in Ethiopia: rainy season locally called *Kiremit* (usually from June to September), dry season locally called *Bega* (October to January), and short rainy season locally called *Belg* (February to May). Camberlin (1997) reported that the Indian monsoon activity is a major cause for summer rainfall variability in the East African highlands. The main rainfall season over the study area starts in June and ends in October. Majority of the study area receives rain during this summer season. The rest of the time it remains relatively dry and hot. The spatial variability of rainfall attributed to altitudinal differences is significant.

For this study, five "class I" stations with different climatic settings distributed over Ethiopia have been selected (Fig. 16.1). The rainfall distribution follows altitude; Dire Dawa has the lower elevations and very hot and dry climatic setting which receives the lowest mean annual rainfall of 661 mm with a standard deviation of 163.6 among the stations, whereas Debre Markos has the highest elevation and relatively cold climatic setting which receives higher annual rainfall of 1,476.8 mm with a standard deviation of 447.6 with extended unimodal type of rainfall. The Bahir Dar station receives the highest rainfall among the stations considered with medium altitude with unimodal rainfall characteristics. Awassa is located in the rift valley region of Ethiopia with bimodal rainfall characteristics, and Dire Dawa is representing lowlands and hot climatic settings. While the Addis Ababa station represents the central highlands, Debre Markos and the Bahir Dar stations represent north and northwest highlands of Ethiopia. The detailed characteristics of the stations are shown in Table 16.1. The Fogera floodplain is located in northwestern Ethiopia, about 625 km from the capital Addis Ababa along the shores of Lake Tana. The Ribb and Gumara rivers with catchment areas of 1,283 and 1,302 km^2, respectively (Abeyou 2008), pass through the plain and both drain into Lake Tana. Total annual rainfall in the floodplain ranges from about 1,100 to 1,530 mm. The mean monthly temperature of the area is about 19 °C. The floodplain is bounded by Lake Tana in the west, the Gumara River in south, the Ribb River in the north, and the Bahir Dar–Gondar road in the east. Its latitude ranges from 11°45′N to 12°03′N, while its longitude lies between 37°29′E and 37°49′E. It stretches about 15 km east–west and 34 km north–south, with an elevation of about 1,800 m above mean sea level (amsl), having an inundation area of about 490 km^2.
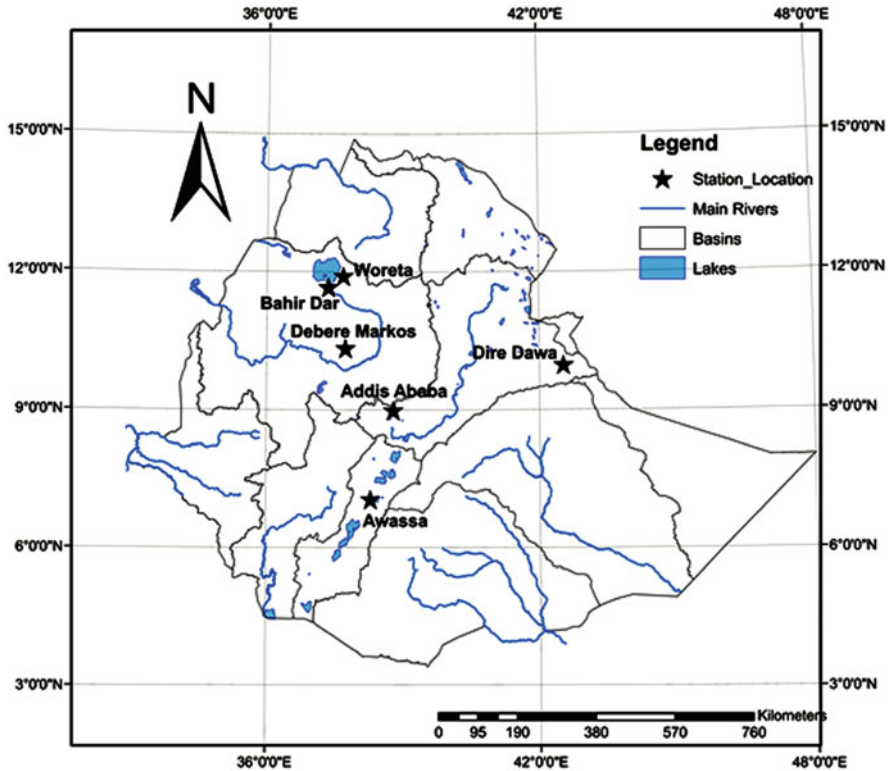
Fig. 16.1 Location map of study area

16.3 Materials and methods

16.3.1 Materials

16.3.1.1 Remote-Sensing Data

From Moderate Resolution Imaging Spectroradiometer (MODIS) onboard *Terra,* instantaneous images and composite products were used for the estimation of energy fluxes in the Fogera floodplain. The 8-day composites of reflectance (MOD09A1), leaf area index (MOD15A2), and the daily land surface temperature (MOD11A1) products were collected from MODIS collection 5. Instantaneous images (MOD021KM) and its respective geo-location files (MOD03) were acquired from Level 1 and Atmosphere Archive and Distribution System (LAADS). With respect to this, MODIS atmospheric products of aerosol optical depth, water vapor content, and ozone content were also collected.

Table 16.1 Station information and data statistics

Station name	Altitude (m)	Rainfall (mm)		Percentage of rainfall in		Type of rainfall	T_{max}		T_{min}		T_{mean}		Number of years
		Mean	Std. dev.	Kiremit	Belg		Mean	Std. dev.	Mean	Std dev	Mean	Std. dev.	
Addis Ababa	2,330	1,219.0	188.6	75.3	20	Bimodal	23.8	2.3	10.3	2.4	17.1	1.6	11
Awassa	1,750	996.2	128.4	44.5	31	Bimodal	27.4	2.5	12.9	2.7	20.1	1.4	11
Bahir Dar	1,800	1,526.9	156.6	93.4		Unimodal	27.2	2.5	12.5	3.2	19.8	2.1	14
Debre Markos	2,446	1,476.8	447.6	81.0		Extended Unimodal	22.9	2.8	10.6	1.9	16.8	1.7	10
Dire Dawa	1,180	661.0	163.6	52.4	34	Bimodal	32.4	2.8	19.1	3.3	25.7	2.8	11

16.3.1.2 Micrometeorology

A field campaign was arranged that installed eddy flux tower in the floodplain, from September 22 to 29, 2008; the eddy flux tower was mounted with: sonic anemometer (CSAT3, Campbell Scientific Inc., Logan, UT, USA), net radiometer (CNR1, Kipp & Zonen, Deft, The Netherlands), and humidity and temperature sensors. These sensors were connected to the Campbell Scientific data logger (CR5000). Wind speed in three directions and the sonic temperature were measured at 20 Hz with the CSAT3, the incoming and outgoing solar radiation, and longwave radiation were measured at 1/3 Hz with CNR1, and temperature and relative humidity data were collected from the CR5000 data logger. The 5-min net radiometer, relative humidity, and air temperature data were also recorded.

16.3.1.3 Meteorological Data

Long-term (10–15 years) daily meteorological data were collected from five "class I" stations from National Meteorological Agency of Ethiopia. Five minutes time resolution weather data were also collected from automatic recording weather station in the floodplain installed in June 2008. These stations were selected for their different ecosystems.

16.3.2 Methods

16.3.2.1 Remote-Sensing Methods

From MODIS onboard *Terra,* products were used for the estimation of ETa in the Fogera floodplain using the Surface Energy Balance Systems (SEBS) algorithms. MODIS detectors measure in 36 spectral bands between 0.405 and 14.385 µm and acquire data at three spatial resolutions of 250, 500, and 1,000 m. MODIS wide spectral resolution and viewing swaths, and atmospherically corrected products make measurements useful in a wide variety of earth system science disciplines. MODIS products of: the 8-day composite surface reflectance, the 8-day composite leaf area index, and daily land surface temperature, were acquired from collection 5. Fractional vegetation cover, broad band albedo, and emissivity were retrieved from SEBS algorithms.

Images Used in the Analysis During the growing season, two images per month were evaluated, and the rest of the year one image per month was considered. Table 16.2 shows the type, date, and Day of the Year (DOY) of the all images evaluated in this study.

Surface Energy Balance Systems (SEBS) Algorithm SEBS is one of the remote-sensing (RS) methods to estimate turbulent surface energy fluxes, developed by

Table 16.2 Date and type of images used in the analysis

Sr. no.	Date	Product name	DOY	Type of product
1	01 January 2008	MOD09A1	1	8-day composite
		MOD15A2		8-day composite daily
		MOD11A1		
2	25 February 2008	MOD09A1	56	8-day composite
		MOD15A2		8-day composite daily
		MOD11A1		
3	28 March 2008	MOD09A1	88	8-day composite
		MOD15A2		8-day composite daily
		MOD11A1		
4	26 April 2008	MOD09A1	111	8-day composite
		MOD15A2		8-day composite daily
		MOD11A1		
5	15 May 2008	MOD09A1	136	8-day composite
		MOD15A2		8-day composite daily
		MOD11A1		
6	25 June 2008	MOD09A1	161	8-day composite
		MOD15A2		8-day composite daily
		MOD11A1		
7	7 July 2008	MOD09A1	189	8-day composite
		MOD15A2		8-day composite daily
		MOD11A1		
8	25 July 2008	MOD09A1	207	8-day composite
		MOD15A2		8-day composite daily
		MOD11A1		
9	8 August 2008	MOD09A1	221	8-day composite
		MOD15A2		8-day composite daily
		MOD11A1		
10	23 August 2008	MOD09A1	236	8-day composite
		MOD15A2		8-day composite daily
		MOD11A1		
11	6 September 2008	MOD09A1	250	8-day composite
		MOD15A2		8-day composite daily
		MOD11A1		
12	22 September 2008	MOD02	266	Instant images
		MOD03		
13	29 September 2008	MOD02	273	Instant images
		MOD03		
14	7 October 2008	MOD09A1	282	8-day composite
		MOD15A2		8-day composite daily
		MOD11A1		
15	14 November 2008	MOD09A1	319	8-day composite
		MOD15A2		8-day composite daily
		MOD11A1		
16	7 December 2007	MOD09A1	341	8-day composite
		MOD15A2		8-day composite daily
		MOD11A1		

Su (2002). MODIS spectral products and meteorological data were used for the estimation of energy fluxes in SEBS. ETa is estimated as a residue of mass balance and energy balance equations in SEBS, which is written as

$$ETa = \frac{R_n - G - H}{\lambda} \tag{16.1}$$

where ETa is the actual ET (mm/day), R_n is the net radiation (MJ/(m^2-day)), G is the soil heat flux (MJ/(m^2-day)), H is the sensible heat flux (MJ/(m^2-day)), and λ is the latent heat of evaporation (J/kg). Parameterizations of the inputs for the SEBS algorithm are explained in detail in Su (2002) and Enku (2009). SEBS uses spectral satellite observations and climatological data for the estimation of energy fluxes. The Woreta and the Bahir Dar weather station data were used. These are solar radiation, air temperature, wind speed, and computed specific humidity. The atmospheric pressure was assumed constant. The calculated instantaneous values were first extrapolated to daily values assuming that the evaporative fraction is constant during the day. Secondly, the daily values were extrapolated to monthly estimates, using the monthly PM estimates based on sunshine hours. All pixels of the floodplain are then averaged to obtain a single monthly ETa value.

16.3.2.2   Micrometeorology

During the field campaign, an eddy flux tower was installed in the floodplain and measurements were made with the sensors mounted on the flux tower. The sonic anemometer (CSAT3) measures at a frequency of 20 Hz and the net radiometer at a frequency of 1/3 Hz. Sensible heat flux and the friction velocity were calculated at half-hourly intervals from eddy covariance data.

Sensible Heat Flux and Friction Velocity From the eddy flux data, sensible heat flux (H), friction velocity (u_*), and the mean wind speed in the three orthogonal directions were calculated with an open source ECPACK software. From the sonic anemometer's wind speed and sonic temperature measurement, sensible heat flux was calculated as

$$H = \rho_a c_p \overline{w' T'} \tag{16.2}$$

where H (W/m^2) is the sensible heat flux, ρ_a (kg/m^3) is the density of the air, c_p (J/kg K) is the specific heat capacity of the air, and $\overline{w' T'}$ is the covariance between the fluctuations of vertical wind speed and the sonic temperature. Friction velocity is a measure of the intensity of turbulence in the planetary boundary layer. This is calculated as

$$u_* = \left(-\overline{v' w'} \right)^{1/2} \tag{16.3}$$

where u_* (m/s) is the friction velocity, v' (m/s) is the horizontal instantaneous velocity fluctuation from the average, and w' (m/s) is the vertical instantaneous velocity fluctuation from the average.

   Sensible heat flux was also calculated from ground measurements of vegetation height and radiometric surface temperature as

$$H = -\rho_a c_p \frac{(T_a - T_s)}{r_{ah}}$$ (16.4)

where H is the sensible heat flux (W/m^2), T_a is the air temperature (K), T_s is the radiometric surface temperature (K), and r_{ah} is the aerodynamic resistance for heat transfer (s/m). The sensible heat flux from the eddy flux tower was also compared with the RS estimations. This is well explained in Enku (2009).

Evaporative Fraction Evaporative fraction is defined as the ratio of latent heat flux to the available energy.

$$\Lambda = \frac{\lambda E}{R_n - G}$$ (16.5)

where Λ is the evaporative fraction, $\lambda E = (R_n - G - H)$ is the latent heat flux (W/m^2), R_n is the net radiation (W/m^2), G is the soil heat flux (W/m^2), and H is the sensible heat flux (W/m^2) determined from equation. The CNR1 radiometer measures incoming and outgoing solar radiation, and longwave radiation, from which the net radiation was calculated.

Surface Albedo The measured incoming and outgoing solar radiation was used for the instantaneous albedo and daily albedo computations. The instantaneous albedo computed from SEBS routines during the satellite overpass was compared with the daily albedo observed CNR1 measurement. This comparison was based on pixel level at the eddy flux tower.

16.3.2.3 Conventional Methods

Information on ET, or consumptive use of water, is significant for water resources planning and management. In this study, different ET estimating models were evaluated with the standard PM method in different ecosystems of Ethiopia. The models were: simple Enku's (E) temperature method, simple Abtew (A) equation, modified Makkink (MM) method, and Priestley–Taylor (PT) method. The performance of these models in different ecosystems will be evaluated with the globally accepted standard PM method.

Penman–Monteith (PM) Method The PM equation (Monteith 1965; Penman 1948) is a physically based combination approach that incorporates energy and aerodynamic considerations. The PM equation produces direct estimates of ETa but requires knowledge of the PM canopy resistance (Sumner and Jacobs 2005). Generally PM equation gives acceptable ET estimates for practical applications in different climatic settings. The method requires inputs of net radiation, soil heat flux, air temperature, relative humidity, and wind speed. The calculation of the net radiation and assumption of soil heat flux were following the FAO-56 methodology. ETo

is the potential ET from a hypothetical green grass of uniform height, 0.12 m, well watered, and a constant albedo of 0.23 with fixed surface resistance of 70 s/m (Allen 1998). PM is considered as a global standard method (Bois et al. 2008; Dingman 2002; Rana and Katerji 2000) and widely used globally. For the reference crop, after the aerodynamic resistance, $r_a = 208/u_2$ and the surface resistance $r_s = 70$ s/m are estimated; the general PM equation can be rewritten as

$$ET_o = \frac{0.408\Delta(R_n - G) + \gamma \frac{900}{T+273}u_2(e_s - e_a)}{\Delta + \gamma(1 + 0.34u_2)} \qquad (16.6)$$

where ETo is the reference ET (mm/day), R_n is the net radiation at the crop surface (MJ/m^2-day), G is the soil heat flux density (MJ/m^2-day), assumed to be zero, on a daily basis, T means the daily air temperature at 2 m height (°C), u_2 the wind speed at 2 m height (m/s), e_s the saturation vapor pressure (kPa), e_a the actual vapor pressure (kPa), e_s the e_a saturation vapor pressure deficit (kPa), Δ the slope of vapor pressure curve (kPa/°C), and γ the psychrometric constant (kPa/°C). The detailed computations of each input for ETo are found in the FAO-56 book. Sensitivity analysis of PM ETo to its input variables was also evaluated.

Enku Simple Temperature Method The Enku simple empirical temperature method (Enku and Melesse, 2013) estimates ETo from only maximum temperature data as

$$ET_o = \frac{(T_{max})^n}{k} \qquad (16.7)$$

where ETo is the reference ET (mm day^{-1}), $n = 2.5$ which can be calibrated for local conditions, $k =$ coefficient which can be calibrated for local conditions. The coefficient, k, could be approximated as $k = 48*T_{mm} - 330$, where T_{mm} (°C) is the daily mean maximum temperature.

Abtew Simple Equation This method requires only solar radiation data for the estimation of ET. The method was tested in wetlands and open waters in different places and found to give a comparable result with complex methods (Abtew 1996; Melesse and Nangia 2005; Melesse et al. 2008). Abtew simple equation is defined as

$$ET = k\frac{R_s}{\lambda} \qquad (16.8)$$

where ET is in mm/day and k is taken as 0.53 and could be adjusted according to the local situation (Abtew and Obeysekera 1995).

Modified Makkink Method The modified Makkink is a modified PT equation, which uses incoming solar radiation instead of net radiation (Brutsaert 2005). This method is one of the simplest radiation models: It requires only average air temperature and the incoming solar radiation. In the same way, this will be compared

with the PM method in different climatic settings. The modified Makkink method is defined as (De Bruin 1981):

$$ET_o = 0.65 \frac{\Delta}{\lambda(\Delta + \gamma)} R_s \tag{16.9}$$

where R_s is the incoming solar radiation MJ/(m^2-day).

Priestley–Taylor Method The Priestley–Taylor (PT) (1972) estimation in different ecosystems will be evaluated with the PM method. The PT equation requires net radiation, soil heat flux, and air temperature. It is expressed as

$$ET_o = \alpha \left(\frac{\Delta}{\Delta + \gamma} \right) \left(\frac{R_n - G}{\lambda} \right) \tag{16.10}$$

where the coefficient α varies in the range of 1.27–1.33; here, we took α as 1.3, ETo in mm/day, and input parameters as mentioned in Eq. (16.6).

16.3.2.4 Penman–Monteith Sensitivity Analysis

A sensitivity analysis is an important technique to improve understanding of the dominant climatic variables in the estimation of ETo in an area of interest. ETo is a measure of evaporative power of the atmosphere. It is independent of the crop type, the age of the vegetation, and management practices. This could be estimated from the meteorological data only. Sensitivity of ETo to the input variables varies with space and time (Gong et al. 2006). "In humid climate, ETo provides an upper limit for actual ET and in an arid climate it indicates the total available energy for actual ET" (Gong et al. 2006). Sensitivity analyses of PM ETo to the inputs—incoming solar radiation, air temperature, relative humidity, and wind speed—were made. Monthly averages of these weather variables were considered. These were increased and decreased by 10, 20, and 30 % from the average value of these variables for each run. To avoid nonsense computations in the sensitivity analysis, minimum and maximum temperature and relative humidity, the average air temperature and relative humidity, and their amplitudes were calculated (Bois et al. 2008). The minimum and the maximum values were taken under considerations while sensitivity for these variables was done. For the computations of net radiation, solar angles at the 15th day of each month were used. In this analysis, it was assumed that the maximum and minimum temperature and relative humidity increase and decrease simultaneously in the analysis of the respective variables.
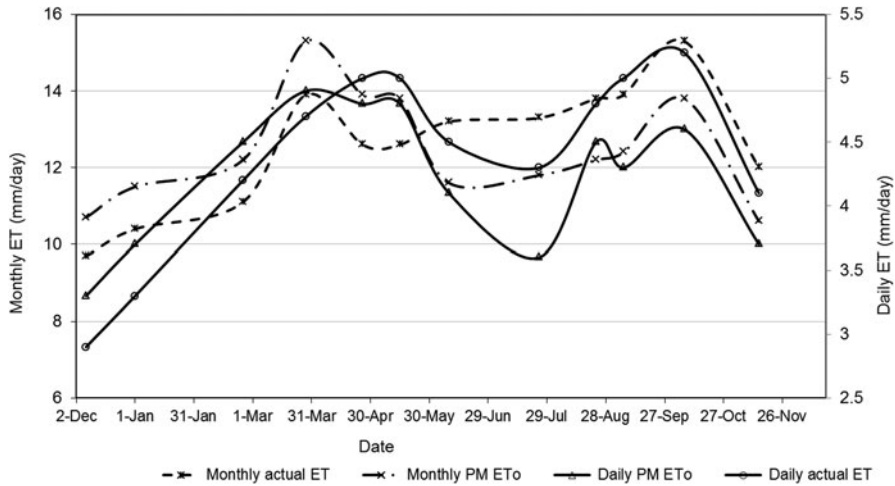
Fig. 16.2 Daily actual ET and PM ETo and monthly actual ET and PM ETo

16.4   Results and Discussion

16.4.1   Remote Sensing (RS)

16.4.1.1   Comparison of Actual ET to PM ETo

ETo is a climatologic variable characterizing the evaporative demand of the surface, whereas ETa represents the effects of soil moisture, land cover heterogeneity, and the variability of climatic conditions. Comparing ETa to ETo gives insight into the spatial variability of land cover and stress conditions. Differences between time series of ETa and ETo for specific crops indicate the seasonal cycle for the crop coefficient. It is noted that differences are also due to possible effects of water stress that is unaccounted for. We assume that water is sufficiently available not to constrain evapotranspiration. We note that ET estimations are for the wet season where rainfall commonly occurs in heavy daily showers. When comparing RS-based ETa with ground-based ETo, one should realize that ETo estimates are spatially limited and computed on a daily basis, whereas the RS technique estimates of ETa are spatially distributed, but they are only valid for the instantaneous time of the satellite overpass. Time series of ETo and ETa are shown in Fig. 16.2. One day per month was analyzed. The instantaneous RS ETa estimates were extrapolated to daily and monthly values.

The annual ETa estimated from this approach was 1,519 mm, while PM ETo was 1,498 mm in the year 2008. The mean annual rainfall over the past 5 years in the Fogera floodplain was 1,296 mm (Enku 2009). This indicates that the annual ETa was about 17 % higher than the mean annual rainfall over the area. This is probably due to the spate irrigation practices in the area during the dry seasons, which use
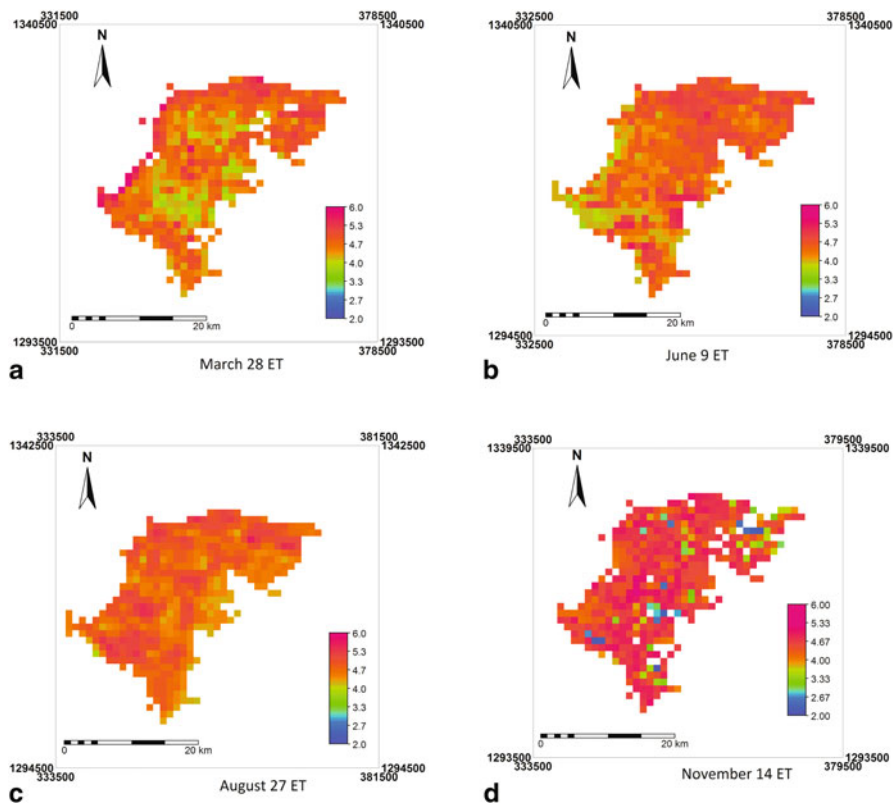
Fig. 16.3 Spatio-temporal distribution of ET over the Fogera floodplain in March (**a**), June (**b**), August (**c**), and November (**d**)

water from upstream areas. In Fig. 16.2, both the RS daily and monthly ETa and the PM ETo daily and monthly estimations follow a similar trend. In the wet season (July–September), the daily estimations from ETa were larger than the respective PM ETo, whereas in dry seasons, the PM ETo was larger than SEBS estimations. This could be explained by the drying out of the top soil layers leading to a reduction of moisture available for evapotranspiration. ETa was limited by the available net radiation during the rainy season.

16.4.1.2 Spatio-Temporal Distribution of ETa over the Floodplain

The spatio-temporal variation of ET in the Fogera floodplain was analyzed using four selected images. The spatial variation over the floodplain was more pronounced in the dry seasons than wet season. The spatial and temporal variations of ET are shown in Fig. 16.3 for selected months. On 27 August 2008 (Fig. 16.3c), the ETa over the floodplain ranges from a minimum value of 3.9 mm to a maximum of about

Table 16.3 Latent heat flux comparison with PM ETo

Date	Sensible heat flux MJ/(m^2-day)	Net radiation MJ/(m^2-day)	Latent heat flux (mm/day)	PM ETo (mm/day)	Kc
23 September 2008	2.045	15.0	5.29	4.58	1.15
24 September 2008	1.813	13.66	4.84	4.33	1.12
28 September 2008	2.831	15.74	5.27	4.81	1.10
Average	2.23	14.8	5.13	4.57	1.12

5.6 mm in forest and water bodies, with a mean value of 4.8 mm and a standard deviation of 0.5 mm. The lower standard deviation here clearly shows that the spatial variation in wet months is less pronounced. Similarly, on 14 November 2008, the spatial distribution of ET follows similar pattern as of 27 August 2008, except here more pixels become drier. Here, the minimum ET was as low as 2.09 mm and the maximum was 5.25 mm a day, with a mean of 4.12 mm and a standard deviation of 0.78 mm as shown Fig. 16.3d.

On 28 March 2008 (Fig. 16.3a), daily ET ranges from a minimum of 3.7 mm to a maximum of 6 mm with a mean value of 4.9 mm and a standard deviation of 0.7 mm. On 9 June 2008 (Fig. 16.3b), daily ET ranges from a minimum of 3.6 mm to a maximum of 5.3 mm with a mean value of 4.4 mm and a standard deviation of 0.5 mm.

16.4.2   Micrometeorology

Here sensible heat flux, latent heat flux, evaporative fraction, and broad band albedo computed from ground observations were compared with the RS derivations.

Sensible Heat Flux   Sensible heat flux computed from the sonic anemometer was compared with the SEBS derived sensible heat flux estimations. The SEBS-derived sensible heat flux comparison was done, both with pixel value and averages of five pixels around the eddy flux tower. The average of the five pixels from SEBS estimation on 22 September 2008 was 119 W/m^2, while the eddy covariance sensible heat flux was 111 W/m^2. On the same day, a pixel value of SEBS sensible heat flux was 123 W/m^2. On 29 September 2008, the average was 107 W/m^2 and the pixel value was 116 W/m^2, while the Eddy covariance sensible heat flux was 82 W/m^2.

Latent Heat Flux   The daily latent heat flux was computed from the eddy flux tower observations. This was compared with the PM ETo. Table 16.3 shows that the PM ETo was less by about 12 %. This difference was comparable with the literature value of the rice crop coefficient during its mid-development stage (Allen 1998); as rice was the dominant crop around the eddy flux tower. Unfortunately, there were no good satellite images during these days and comparing with the RS estimations was not possible.

Evaporative Fraction   The instantaneous evaporative fraction derived from RS technique was compared with evaporative fraction computed from the eddy flux

Table 16.4 Comparison of instantaneous and daily evaporative fraction

Date	Evaporative fraction			
	Instantaneous		Daily	Diff (%)
	From satellite data	Eddy flux data		
22 September 2008	0.75	0.76	–	–
23 September 2008	–	0.79	0.89	11.54
24 September 2008	–	0.79	0.88	10.38
28 September 2008	–	0.70	0.83	15.00
29 September 2008	0.77	0.71	–	–

Table 16.5 Instantaneous and daily albedo computed from the CNR1 observations

Date	Instant albedo at satellite overpass	Daily albedo	Percentage increase (%)
23 September 2008	0.13	0.15	15.4
24 September 2008	0.13	0.15	15.4
28 September 2008	0.13	0.15	15.4
Average	0.13	0.15	15.4

tower at the time of satellite overpass. The evaporative fraction from SEBS algorithm was found comparable with the eddy flux tower computation. These instant values were also compared with the daily average values computed from the eddy flux measurement. It was found that the instantaneous evaporative fraction was less by an average of about 12 %. The daily evaporative fraction was found constant except at the sunrise and sunset, where it was unstable. The detail is shown in Table 16.4.

Surface Albedo   The instantaneous surface albedo during the satellite overpass computed from the eddy flux tower was compared with the daily average. It was found that the instantaneous albedo was about 15 % lower than the daily albedo. This was applied to adjust the instantaneous values to the daily estimates in the RS technique, which improves the RS ET estimations over the floodplain. The instantaneous and the daily computed albedo are shown in Table 16.5.

16.4.3   Conventional Methods

The ETo estimations of the different conventional methods were compared with the PM estimations, and the performances of these methods against the PM method were evaluated in different ecosystems. The performances of these methods were evaluated using four indices: coefficient of determination (R^2), Nash–Sutcliffe efficiency (NSE), absolute mean error (AME), and root mean square error (RMSE) values. The detailed performances of the methods with different ecosystems are as shown in Table 16.6. The methods show different performances in different ecosystems. The MM method performs very well without local calibration of the model coefficient, in most objective functions set and in all stations except the Dire Dawa

Table 16.6 Comparison results of different methods with PM

Station and period	Methods	Performance when compared with PM				Percentage error
		R^2	NSE	AME	RMSE	
Addis Ababa (1995–2005)	E	0.61	0.52	0.40	0.51	2.5
	A	0.9	0.72	0.31	0.39	7.7
	MM	0.94	0.88	0.21	0.26	3.4
	PT	0.91	0.9	0.18	0.23	0.67
Awassa (1995–2005)	E	0.58	0.3	0.44	0.55	0.32
	A	0.89	0.64	0.31	0.39	7.11
	MM	0.93	0.88	0.18	0.23	1.22
	PT	0.89	0.89	0.17	0.22	1.31
Bahir Dar (1998–2011)	E	0.63	0.52	0.42	0.55	19
	A	0.7	0.58	0.41	0.51	13.8
	MM	0.79	0.79	0.27	0.36	18.6
	PT	0.76	0.72	0.30	0.42	22
Debre Markos (2002–2011)	E	0.7	0.69	0.5	0.6	3.5
	A	0.77	0.7	0.4	0.5	5.9
	MM	0.84	0.83	0.3	0.38	2.2
	PT	0.66	0.65	0.4	0.54	1
Dire Dawa (1995–2005)	E	0.67	0.66	0.54	0.70	0.1
	A	0.32	0.22	0.82	1.06	6.9
	MM	0.47	0.03	0.86	1.18	15.4
	PT	0.56	0.55	0.62	0.81	1.5

E Enku simple temperature, *A* Abtew simple equation, *MM* Modified Makkink, *PT* Priestley–Taylor

station. Dire Dawa has hot and dry climatic setting, where the performances of MM, A, and PT methods were poor. In this station, the E simple temperature method is performing well. Calibrating the coefficient of A equation improves the performance of the method in all the stations as shown in Table 16.6. Locally calibrated coefficient at the Dire Dawa station did not bring about significant performance improvement. Figure 16.4 shows the scatter plots of the different methods with the PM approach at Debre Makros station.

Enku Simple Temperature Method The estimation of ETo with this simple method was compared with the PM estimations, and the performance was evaluated. The method performed well in the majority of the stations with R^2, NSE, AME, and RMSE of 0.7, 0.69, 0.5, and 0.6 respectively, at Debre Markos station. The method also performs better than any other methods tested at the Dire Dawa climatic setting in all performance criteria used. The details are as shown in Table 16.6.

Abtew Simple Equation In the same way, the estimation of the method was also compared with the PM estimations and its performance in different ecosystems was evaluated. The method performs well after the coefficient was locally calibrated, in almost all the criteria set in all stations except the Dire Dawa station, where it fails to estimate ET properly as shown in Table 16.6.

Modified Makkink Method The MM method performs very well in all the performance evaluation criteria in all the stations except Dire Dawa station without
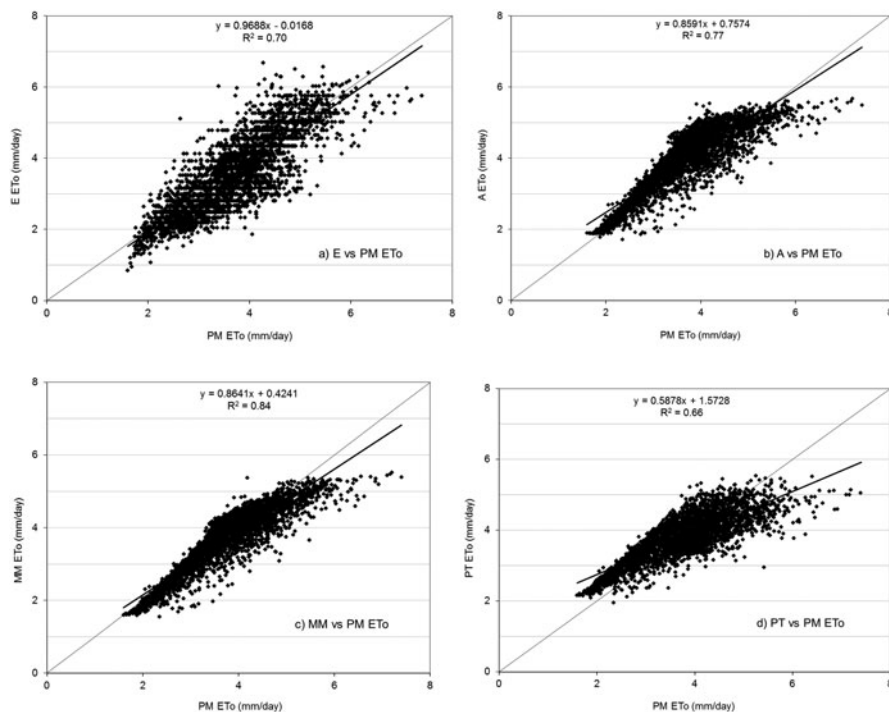
Fig. 16.4 Scatter plots of different methods with PM ETo at Debre Markos station

calibrating the coefficients. It performs very well, especially at the Addis Ababa station with R^2, NSE, AME, and RMSE of 0.94, 0.88, 0.21, and 0.26, respectively. MM was developed for wet surfaces; as a result, it will not be a surprise that the MM method is not performing well in dry and hot climatic setting like Dire Dawa as shown in Table 16.6.

Priestley–Taylor Method   PT method is also performing well in most of the climatic settings, but it requires local calibration of the coefficient as low as 1.1 in most stations that brought about significant performance improvement at Addis Ababa, Awassa, and Bahir Dar stations. Locally calibrated coefficient at the Dire Dawa station did not bring about significant performance improvement.

16.4.4   Sensitivity Analysis

Sensitivity analysis of the PM ETo for its input variables was done in the year 2007 at Bahir Dar station. The result of sensitivity analysis showed that solar radiation was found the most sensitive weather variable almost independent of the seasons of the year. PM ETo was also comparably sensitive to air temperature as solar radiation.

Table 16.7 Weather variables statistics at Bahir Dar station

	T_{max} (°C)	T_{min} (°C)	T_{mean} (°C)	RH (%)	SS (h)	Rs (MJ/m²-day)	WS (m/s)
Mean	27.2	12.5	19.8	57.9	8.0	20.5	0.9
Std. dev.	2.4	3.2	2.1	15.6	2.8	3.8	0.4

T_{max} maximum temperature, T_{min} minimum temperature, T_{mean} mean temperature, *RH* relative humidity, *SS* sunshine hours, *Rs* incoming solar radiation, *WS* wind speed
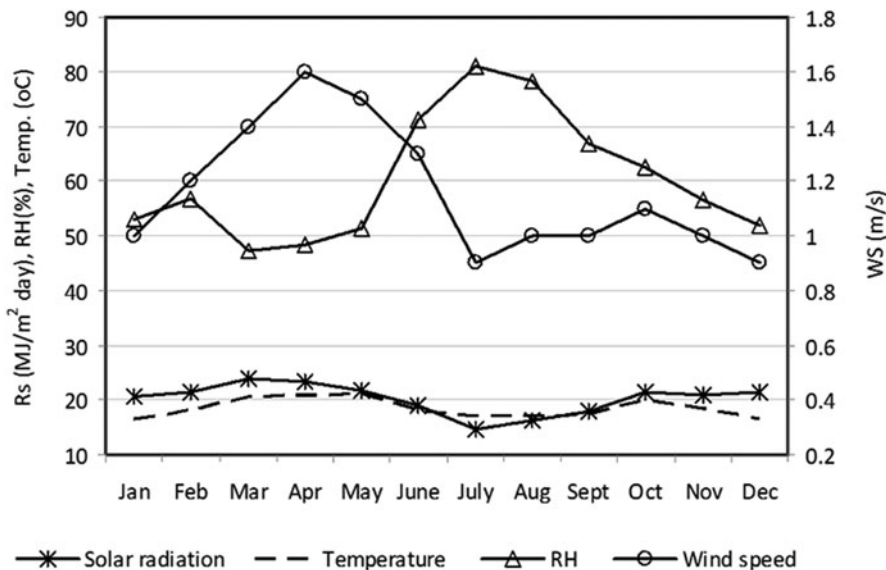
Fig. 16.5 Monthly average weather variables at the Bahir Dar station (2007)

Wind speed was found least sensitive. Relative humidity influences ETo negatively and high relative humidity values have more influence on ETo than smaller values. Gong et al. (2006) explained sensitivity of ETo to the input variables varies with seasons. But here sensitivity result does not change with the change of seasons. This is because the variation of weather variables for more than a year is a minimum in the area. For example, the long-term mean wind speed in the area was 0.9 m/s with a standard deviation of 0.4 m/s. The long-term (14 years) mean and standard deviation of the weather variables at Bahir Dar station are shown in Table 16.7.

During the sensitivity analysis, long-term weather data were evaluated. The daily maximum and minimum solar radiation was 27.53 MJ/(m²-day) and 8.9 MJ/(m²-day) in April and October, respectively. The daily maximum and minimum temperature was 33.8 °C in April and December 0 °C, respectively. The relative humidity ranges from a minimum of 21 % to a maximum of 94 %. Minimum was in April and maximum was in July, August, and September. The monthly average weather variables at Bahir Dar station is shown in Fig. 16.5.
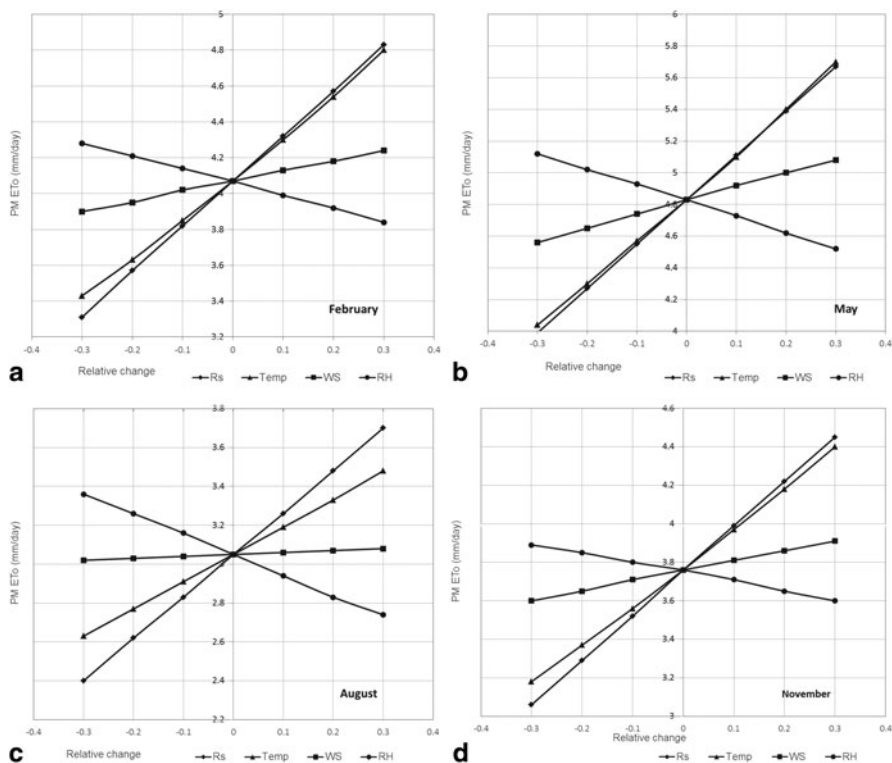
Fig. 16.6 Sensitivity analysis results of ETo to input variables in February (**a**), May (**b**), August (**c**), and November (**d**)

A simple but practical way of presenting a sensitivity analysis is to plot relative changes of weather variables against changes in PM ETo as a curve. The sensitivity analysis result at Bahir Dar station for some months in the year 2007 representing different seasons is shown in Fig. 16.6.

16.5   Conclusions and Recommendations

The spatial average of ETa estimated from RS over the floodplain was smaller than the PM ETo in relatively drier periods, but greater in wet seasons. This is because the increased biomass in the wet season evapo-transpire at a potential rate and the available soil moisture. The annual ETa over the plain was found to be about 1,519 mm, whereas the annual PM ETo was 1,498 mm. In wet seasons, the spatial variation of ETa was less pronounced, whereas in relatively dry months the spatial variation was clearly pronounced. ET estimation from remote-sensed inputs have generally been improved.

Ground Ground-based estimations of ETo for the long-term time series data were done using different methods at five different ecosystems distributed over Ethiopia. The different empirical methods were compared to the standard PM ETo. From the different conventional methods used, the MM method was the only method which does not require local calibration of the coefficient to perform best in all the stations except Dire Dawa station where its performance was poor. This method performed the best among the models tested, with an R^2 of 0.94, NSE of 0.88, RMSE of 0.26 mm, and AME of 0.21 mm at Addis Ababa and Awassa stations. The PT method overestimated ETo when the a priori coefficient, $\alpha = 1.3$, was used. Estimates were improved well when the coefficient α was reduced to 1.1 in most of the stations considered. The simple Abtew equation also performed well in the area. However, it proved necessary to calibrate the coefficient.

Radiation and temperature were found almost equally sensitive inputs to the PM ETo almost irrespective of the seasons. That was why Enku's simple temperature method was performing well in the stations used in this study consistently. This method performs well, even at the Dire Dawa station where other methods failed. This method is recommended for the area where there is insufficient data to use other methods, especially for annual ET estimations for hydrological studies. The results obtained with the MM and A methods appear to be promising. However, calibration of the a priori coefficients is required before these simple methods can be routinely applied in the area. Application of these simple methods in dry and hot ecosystems in the area should be seen in cautiously.

References

Abeyou W (2008) Hydrological balance of Lake Tana upper Blue Nile basin, Ethiopia, ITC, Enschede, p 94

Abtew W (1996) Evapotranspiration measurements and modeling for three wetland systems in South Florida. Water Resour Bull 32(3):465–473

Abtew W, Obeysekera J (1995) Lysimeter study of evapotranspiration of cattails and comparison of three estimation methods. In: Transactions of the American society of Agricultural Engineers ASAE, 38 (1995) 1, pp 121–129

Allen RG (1998) Crop evapotranspiration: guidelines for computing crop water requirements. FAO irrigation and drainage paper; 56. FAO, Rome, p 300

Bois B, Pieri P, Van Leeuwen C, et al (2008) Using remotely sensed solar radiation data for reference evapotranspiration estimation at a daily time step. Agric For Meteorol 148(4):619–630

Brutsaert W (2005) Hydrology: an introduction. Cambridge University Press, Cambridge, p 605

Camberlin P (1997) Rainfall anomalies in the source region of the Nile and their connection with the Indian Summer Monsoon. J Clim 10:1380–1392

De Bruin HAR (1981) The determination of (reference crop) evapotranspiration from routine weather data. Proc Inform Community Hydrol Res TNO. The Hague 28:25–37

Dingman SL (2002) Physical hydrology. Prentice Hall, Upper Saddle River

Enku T (2009) Estimation of evaporation from satellite remote sensing and meteorological data over the Fogera floodplain, Ethiopia, Enschede, MSc thesis ITC, p 89

Enku T, AM Melesse (2013) A simple temperature method for the estimation of evapotranspiration. Hydrol Process. doi:10.1002/hyp.9844

Gong L, Xu CY, Chen D et al (2006) Sensitivity of the Penman-Monteith reference evapotranspiration to key climatic variables in the Changjiang (Yangtze River) basin. J Hydrol 329(3–4):620–629

Monteith JL (1965) Evaporation and surface temperature. Quart J R Meteorol Soc 107:1–27

Melesse AM, Nangia V (2005) Estimation of spatially distributed surface energy fluxes using remotely-sensed data for agricultural fields. Hydrol Process 19(14):2653–2670

Melesse AM, Abtew W, Tibebe D (2008) Simple model and remote sensing of evaporation estimation for Rift Valley Lakes in Ethiopia. In: Melesse AM, Abtew W (eds) Hydrology and ecology of the Nile Basin under extreme conditons. Addis Ababa, Ethiopia

Penman HL (1948) Natural evaporation from open water, bare soil, and grass. Proc R Soc London A193:120–145

Priestley CHB, Taylor RJ (1972) On the assessment of surface heat flux and evaporation using large scale parameters. Mon Weather Rev 100(2):81–92

Rana G, Katerji N (2000) Measurement and estimation of actual evapotranspiration in the field under Mediterranean climate: a review. European J Agron 13(2–3):125–153

Su Z (2002) The Surface Energy Balance System (SEBS) for estimation of turbulent heat fluxes. Hydrol Earth Sys Sci 6(1):85–99

Sumner DM, Jacobs JM (2005) Utility of Penman-Monteith, Priestley-Taylor, reference evapotranspiration, and pan evaporation method to estimate pasture evapotranspiration. J Hydrol 308(1–4):81–104